


Please cite the Published Version

Ebrahimzade, Iman, Ebrahimi-Nik, Mohammadali, Rohani, Abbas and Tedesco, Silvia  (2022) Towards monitoring biodegradation of starch-based bioplastic in anaerobic condition: finding a proper kinetic model. *Bioresource Technology*, 347. p. 126661. ISSN 0960-8524

DOI: <https://doi.org/10.1016/j.biortech.2021.126661>

Publisher: Elsevier BV

Version: Accepted Version

Downloaded from: <https://e-space.mmu.ac.uk/628974/>

Usage rights:  [Creative Commons: Attribution-Noncommercial-No Derivative Works 4.0](#)

Additional Information: This is an Author Accepted Manuscript of an article published in *Bioresource Technology*.

Enquiries:

If you have questions about this document, contact openresearch@mmu.ac.uk. Please include the URL of the record in e-space. If you believe that your, or a third party's rights have been compromised through this document please see our Take Down policy (available from <https://www.mmu.ac.uk/library/using-the-library/policies-and-guidelines>)

Towards monitoring biodegradation of starch-based bioplastic in anaerobic condition: finding a proper kinetic model

Iman Ebrahimzade, Mohammadali Ebrahimi-Nik, Abbas Rohani, Silvia Tedesco

PII: S0960-8524(21)02003-4
DOI: <https://doi.org/10.1016/j.biortech.2021.126661>
Reference: BITE 126661

To appear in: *Bioresource Technology*

Received Date: 6 November 2021
Revised Date: 27 December 2021
Accepted Date: 28 December 2021



Please cite this article as: Ebrahimzade, I., Ebrahimi-Nik, M., Rohani, A., Tedesco, S., Towards monitoring biodegradation of starch-based bioplastic in anaerobic condition: finding a proper kinetic model, *Bioresource Technology* (2022), doi: <https://doi.org/10.1016/j.biortech.2021.126661>

This is a PDF file of an article that has undergone enhancements after acceptance, such as the addition of a cover page and metadata, and formatting for readability, but it is not yet the definitive version of record. This version will undergo additional copyediting, typesetting and review before it is published in its final form, but we are providing this version to give early visibility of the article. Please note that, during the production process, errors may be discovered which could affect the content, and all legal disclaimers that apply to the journal pertain.

Towards monitoring biodegradation of starch-based bioplastic in anaerobic condition: finding a proper kinetic model

Iman Ebrahimzade¹, Mohammadali Ebrahimi-Nik^{1*}, Abbas Rohani¹, Silvia Tedesco²

¹Department of Biosystems Engineering, Faculty of Agriculture, Ferdowsi University of Mashhad, Mashhad, Iran,

²Department of Engineering, School of Mechanical Engineering, Manchester Metropolitan University, Dalton Building, Chester Street, Manchester, M1 5GD, UK

Abstract

Bioplastic biodegradation showed varying behavior during the process of biodegradation. The First-order and Gompertz models are the most prevalent models for monitoring biodegradation in an anaerobic digestion (AD) process, which do not suit adequately bioplastics fermentation modeling. This research aimed at studying the kinetics of methane production during AD of starch-based bioplastic by using a large library of non-linear regressions (NLRs) and an artificial neural network (ANN). Although 26 NLR models (25 were outlined in the AD literature + 1 modified by authors) have been analyzed, 9 of them were proper predictors for the whole AD process for methane production. In the end M9, which has been proposed by authors, was selected owing to the simplicity of regression as well as good statistical criteria. Moreover, MLP-ANN could outperform the NLR model and has been selected as the superior model that can define the kinetics of bioplastic AD.

Keywords: Anaerobic Digestion; Bioplastic; Kinetic Study; Modeling

1. introduction

Bioplastics have attracted considerable interest ever since the 1970s (Nair et al., 2017). They supply multiple waste management options and are effective in limiting greenhouse gas emissions by reducing carbon footprint and fossil fuel applications (Shrestha et al., 2020). Bioplastics are not

just a single substance. In fact, they consist of various materials with different properties and applications. Plastic material is defined as bioplastic if it is either biodegradable or biobased or embeds both properties. The term "biobased" means that the substrate originated from biomass, at least to some extent. This biomass can include corn starch, sugarcane, or cellulose (Europeanbioplastics, 2016). Biodegradable polymers in which starch is used either as the main material or as an additive are called starch-based polymers. The starch content of these polymers can vary between 5% and 90% of total weight (Davis & Song, 2006).

The European bioplastics market report reveals a huge growth in the global production capacity of biodegradable bioplastics recently. This capacity is estimated to be increased from 1.2 million tonnes to 1.8 million tonnes by 2025 (Europeanbioplastics, 2020). Due to differences in their composition, these materials showed different behaviors during the process of biodegradation. Consequently to their unknown behaviors, many bioplastics are not digested and lead to environmental pollution hence the management of these materials at the end of life is critical for sustainability (Ryan et al., 2017), and studying their biodegradation should be prioritized. This has drawn researchers' attention to survey the biodegradability of bioplastics under varied aerobic and anaerobic conditions. Among available experimental methods for measuring the biodegradation of polymers (Shah et al., 2008), Anaerobic Digestion (AD) of bioplastics has not received extensive attention (Bátori et al., 2018; Cho et al., 2011). AD produces a reliable form of energy (biogas) with a shorter retention time in comparison to aerobic digestion (Shrestha et al., 2020). Also, AD of bioplastic (PLA) leads to more greenhouse gas savings (Piemonte, 2011). Chemical and physical properties of bioplastics are determinative factors for biodegradation. Hydrophilic nature, surface area, chemical structure and composition, crystallinity, molecular weight and microbial community are among important parameters (Bátori et al., 2018; Muniyasamy et al.,

2017). Among parameters associated with biodegradability of bioplastics, surface area (García-Depraect et al., 2022) and microbial community (Wang et al., 2018; Yagi et al., 2009) have major roles. In this context, however, the particle size (PS) has showed different, and even sometimes conflicting behavior in AD of bioplastics i.e. (Massardier-Nageotte et al., 2006) and (Yagi et al., 2012). The authors have previously reported successful degradation of starch-based bioplastics with 23% energy efficiency (Ebrahimzade et al., 2021). A growing body of literature in this field has focused on higher biogas yield/biodegradation (Shrestha et al., 2020) (i.e. (Mohee et al., 2008; Weiwei et al., 2016; Zhang et al., 2018)) and only a few studies have dealt partially with the kinetics of bioplastic biodegradation. Kinetic analysis helps evaluate the AD performance by obtaining maximum methane production, production rate and lag phase (Andriamanohiarisoamanana et al., 2020).

A striking feature of the First-order and Gompertz models is simplicity which makes them the most prevalent models for monitoring the AD process (Maleki et al., 2018). In the literature, the applicability of 5 kinetic models for anaerobic degradation of poly(hydroxybutyrate-co-hydroxyvalerate) (PHBV) was studied and concluded that the Gompertz model well described the system for PSs larger than 0.8 mm (Ryan et al., 2017). On the other hand, researchers stated the inadequacy of common kinetic models in some AD processes (Andriamanohiarisoamanana et al., 2020). These models are not suitable for complex substrates as well as those affected by inhibition (Ware & Power, 2017). Starch-based bioplastics are partially degraded in AD (Quecholac-Piña et al., 2020) while its starch content undergoes rapid degradation (Russo et al., 2009). Also, some bioplastics contain inorganic materials such as Polypropylene and Polystyrene. Taken as a whole, it can be conceivably hypothesized that the traditional models would not fit adequately to the AD of starch-based bioplastics. In this context, the authors have previously reported that the modified

Gompertz might not be a valid approximator owing to $R^2 = 0.94$ for PS: 4.3, ISR: 4 (Ebrahimzade et al., 2021).

Mathematical modeling of AD is a fast and cost-effective method for the prediction and optimization of fuel processing engineering and waste industry design (Andriamanohiarisoamanana et al., 2020). In this context, non-linear models seem to be compatible with AD processes, since the growth of microorganisms and as a result, the kinetics of production are more often nonlinear (Khamis, 2005). Within this framework, different non-linear regressions (NLRs) were retrieved through AD experiments. The procedure of fitting nonlinear models involves multi-steps. The principal characteristics of nonlinear models are parsimony, interpretability, and prediction. On the other hand, key drawbacks are reduced flexibility compared to linear models and lack of an analytical solution for estimating the parameters. Also, an appropriate selection in a large library of functions is of great importance (Archontoulis & Miguez, 2015). More to the point, samples must be representatively large as well as accurate to obtain the desired results through the regression model. Therefore, this method is highly sensitive and may lead to errors (Wang et al., 2011).

Besides non-linear models, artificial neural networks (ANN) showed magnificent results in biological applications (Abunama et al., 2019; Saghoury et al., 2020). Neural networks can accurately predict biogas production with R^2 from 0.87 to 1 (Guo et al., 2020). ANN matrices have the ability to estimate non-linear relationships existing between independent and dependent variables to a great degree of reliability (Shojaimehr et al., 2014). They are independent of mathematical relationships and perform as a black box (Saghoury et al., 2020). Thus, this method could be a promising alternative for covering NLR disadvantages. One of the most common types of neural networks is the multilayer perceptron (MLP).

Further research is required to elucidate the kinetic model of bioplastic biodegradation. A thorough search of the relevant literature confirms that no study has been carried out on the monitoring methane yields from the AD of starch-based bioplastics using NLRs and ANN. This paper addresses critical knowledge gaps that relate to the rates and performance of bioplastic biodegradation, particularly if starch-based in anaerobic conditions. To reach this ambitious goal, new models have to be developed efficiently considering wide ranges of ISR and PSs. A crucial role in this modeling has been played by “NLRs” and “ANN”. Therefore, this study aimed at i) studying different NLR models and describing models that are proper for monitoring the AD of bioplastics, ii) investigating MLP-ANN as a promising alternative for modeling the bioplastic biodegradation.

2. Material and methods

2.1. Data collection and laboratory experiment

To conduct a kinetic modeling study that could explain the metabolic pathways involved in AD of starch-based bioplastic, 729 data were obtained from the authors’ previous study (Ebrahimzade et al., 2021). AD was performed in mesophilic conditions (37 °C) with three replicates following the steps outlined by Holliger et al. (2016). The average PSs of bioplastics were 0.72, 4.30, and 7.87 mm which were employed in each sample with the following ISRs: 2, 3, and 4 (Table 1). Microcrystalline cellulose (Merck-Germany) was used as a positive control to assess the quality of inoculum (Holliger et al., 2016). The inoculum was supplied from a pilot-scale digester which was fed daily with food waste after the digester achieved a steady state of methane production. The produced biogas was stored in a gas-tight bag that was thoroughly checked for any leak while measuring of methane was performed daily with a syringe according to Stoddard (2010). Then data were normalized as proposed by Nielfa et al. (2015). The applicability of the kinetic model is

preponderantly affected by AD's operational parameters, the type of inoculum, and the compositional properties of the substrates (Andriamanohiarisoamanana et al., 2020). Additionally, the chemical composition of the bioplastics affects biodegradation (Bátori et al., 2018). Thus, the results of elemental analyses, acidity and total solid (TS) of media were reported to facilitate the repeatability of experiment. For this purpose, CHNO and pH analyzes were conducted in the experiment via a Thermo Finnigan (FLASH EA 1112 SERIES) and a digital pH meter (EDT directION RE357) respectively. The substrate was Nooraste® starch-based bioplastic with 0.45 mm thickness that contained about 60% of corn starch. The CHNO analysis showed this substrate contained 53.83% C, 7.81% H, 0.53% N, and 37.83% O. The pH of the inoculum and substrate was approximately 7.4. The TS and volatile solid (VS) were 97.78 and 86.16 for bioplastic, 4 and 71 for inoculum respectively. Finally, the TS of all treatments was adjusted to 5%.

2.2. Kinetic evaluation

In this section, various NLR models and MLP neural networks were used to estimate the methane production from the treatments. Then, based on these models, their methane production process was investigated.

2.2.1. Non-linear regression (NLR)

The use of nonlinear models leads to the estimation of parameters such as degradation rate, the volume of gas resulting from the degradation of each nutrient, and the lag phase of the fermentation process (Schofield et al., 1994). For an NLR model, equation 1 was used to describe the system's behavior.

$$\phi_i = f(t_i, \beta) + \varepsilon_i \quad (1)$$

where f is the response variable (methane production), t is the independent variable (time), β is

the vector of parameters β_j to be estimated ($\beta_1, \beta_2, \dots, \beta_k$), ε_i is a random error term, k is the number of unknown parameters and $i = 1, 2, \dots, n$, is the number of the observation. The estimators of β_j 's were found by minimizing the sum of squares error (Khamis, 2005). Model coefficients were obtained through MATLAB function (fitnlm) which was based on the prediction error minimization by the Levenberg-Marquardt non-linear least-squares algorithm. It became apparent that cumulative gas production profiles vary in shape from steep diminishing returns to highly sigmoidal (France et al., 2000). For this reason, the profiles of cumulative methane yields were fitted with 25 conventional models which were capable of modeling shapes with no inflexion point and sigmoidal shapes with a variable inflexion point (France et al., 2000). Most NLR models, except the exponential ones, are sigmoidal. Among the sigmoid functions, Logistic and Gompertz functions are sigmoid curves with a fixed inflexion point. The logarithmic model also has a fixed inflexion point at half of the final gas volume, while the Generalized Mitscherlich, Richards, and Michael Menten are sigmoidal shapes without fixed inflexion points (Wang et al., 2011; Ware & Power, 2017). In addition, some models with shape parameter were used that would allow flexibility in the fitted curve (Ware & Power, 2017). The authors also provided a new model (M9) consisting in a modified form of Michael Menten's model, which was also much simpler. The one-pool model can be expanded to two-pool analysis, assuming that the potentially degradable substrate consists of fast and slow degradation parts (Wang et al., 2011). Thus, Two-pool exponential (M10) and Two-pool logistic (M11) were used. The remaining models which were obtained from biological studies, had a variety of features for modeling. All of the analyzed NLRs in this study, are detailed in Table 2. a , b , c and d represent model parameters while t stands for the independent variable (time) in the equations described in Table 2.

2.2.2. MLP neural network

MLP is a supervised neural network consisting of several layers of processing components. This network consists of three types of layers i.e. input, hidden, and output (Rohani et al., 2011). The two variables PS and ISR were used as input (independent) variables to estimate the volume of produced methane. In MLP, each neuron communicates with the input layer and output through weights (W_1 & W_2). Structure of MLP-ANN has been illustrated (see supplementary material). The neural network processed the input variables in parallel although the transfer of information from one layer to another was conducted in series.

Train and test are two stages of MLP. Selecting the size of training dataset is a critical consideration. Too much data make the learning process so long following which is overfitting while too few training datasets follow inappropriate learning features, failure in generalization, and poor network performance to unseen patterns (Rafiq et al., 2001). Multiple research proposed several methods (i.e. (Rafiq et al., 2001)) for determining the minimum size of the training data although there is no generic principle in this matter. To fulfill this demand the performance of different sized training datasets has been evaluated. Success in training was measured by an error function (equation 2). During training, weights were according to equation 3 to reduce error, and training ended once the error was minimized. Consequently, the weights were adjusted so that the output of the model was sufficiently close to the target output. In the test phase, an input pattern was applied to the network, and the network calculated the corresponding output. The best results were obtained when the prediction error was minimum in both the training and test stages. The three factors of PS, ISR, and methane production have different ranges of variation. Therefore, in order to have an acceptable performance of the MLP, the data set was normalized in the range [-1.1] using equation 4. This domain of normalization was due to the use of the sigmoid transfer function in latent layer neurons (Rohani et al., 2011).

$$E = \frac{1}{n} \sum_{i=1}^n (V_{pi} - V_{ei})^2 \quad (2)$$

$$W_i = W_{i-1} - \eta \frac{\partial E}{\partial W} \quad (3)$$

$$x_n = \frac{2 \times (x - x_{min})}{x_{max} - x_{min}} - 1 \quad (4)$$

1 V_{pi} and V_{ei} stand for predicted methane volumes and laboratory methane volumes, respectively.
 2 η is the learning rate, x_n is the normalized data, x_{max} and x_{min} are the minimum and maximum
 3 data, and i is the training iteration. 12 training algorithms were used to find the optimal weights
 4 between neurons. These algorithms were from 5 classes of Self-adaptive learning rate (Traingdx,
 5 Traingd), Quasi-Newton (Trainlm, Trainoss, Trainbfg), Bayesian regulation backpropagation
 6 (Trainbr), Conjugate gradient backpropagation (Trainscg, Traincgb, Traincgp, Traincgf), and
 7 Resilient backpropagation (Trainrp). The working steps of MLP-ANN has been demonstrated (see
 8 supplementary material).

9 2.2.3. Comparing the eligibility of models

10 Performance functions were employed to the achieved models to compare their prediction
 11 accuracy. These statistical functions are coefficient of determination (R^2), root mean square error
 12 (RMSE), the total sum of squares error (TSSE) and model efficiency (EF), whose equations are
 13 described by equations (5-8).

$$R^2 = 1 - \sum_{a=1}^N (x_a - \hat{x}_e)^2 / \sum_{a=1}^N (x_a - \hat{x}_e)^2 \quad (5)$$

$$RMSE = \sqrt{\left(\sum_1^N |x_a - \hat{x}_e|^2\right) / N} \quad (6)$$

$$TSSE = \sum_1^N |x_a - \hat{x}_e|^2 \quad (7)$$

$$EF = \frac{\sum_1^N (x_a - \bar{x})^2 - \sum_1^N (\hat{x}_e - x_a)^2}{\sum_1^N (x_a - \bar{x})^2} \quad (8)$$

Where x_a indicates the actual value, \hat{x}_e indicates the estimated value, \bar{x} is the average value and N is the sample size. The selected model should be able to have a zero estimate of the biomethane production at the time point of zero otherwise the kinetic model is biologically unreliable (Wang et al., 2011). Therefore, another criterion was evaluated which was the primary point (PP). The model with high R^2 and EF, low RMSE and TSSE, and PP = 0 was chosen as an appropriate model for predicting the kinetics of methane production.

3. Results and Discussions

3.1. Characteristics of methane yield

The experiment lasted for 26 days and methane yields were achieved in the range of 135 mL $\text{CH}_4/\text{g.VS}$ and 250 mL $\text{CH}_4/\text{g.VS}$ for specimens. Due to the good bioavailability of starch in bioplastic, rapid methane production was perceived. More details were included in the previous research (Ebrahimzade et al., 2021).

3.2. Kinetic evaluation

In this section, the best NLR model was selected from the presented models. Then, the model was used to investigate the kinetics of methane production from experimental treatments. RMSE, R^2 ,

and PP values of 26 NLRs has been calculated (see supplementary material). The most remarkable finding to emerge from NLRs analysis was that only 8 NLRs (including M1, M3, M8, M9, M21, M23, M24, and M25) were sufficiently accurate to estimate the methane production from digestion over time, whereas a good agreement fell through for other NLRs. Because the estimated value of these models at zero time was opposite to zero ($PP \neq 0$), while the models must pass the origin of the coordinate. However, the M17 model could be included among the suitable models' group subject to PP value at T1 and T7 treatments be ignored. Inaccuracy in the initial stage of biodegradation could exacerbate modeling experimentation due to more performance time, longer and non-convergence of the iteration, and possibly convergence to an undesirable local minimum sum of squares residual (Khamis, 2005). Formerly a group of scientists stated that the M5 and M6 models exhibited a considerable gas volume at the initial stages of incubation (Wang et al., 2011). In general, the robustness of models declines as the number of phases increase (France et al., 2000), which is consistent with the results achieved in this study. The R^2 value for M3, M4, M12, M23 and M25 was 0.893, 0.992, 0.987, 0.986 and 0.986 respectively in the PHBV biodegradation study at 37 °C and ISR:1 (Ryan et al., 2017). The fitting results in the current study for M3 were more accurate. Recently Chinaglia et al. (2018) described the enzyme kinetics involved in aerobic biodegradation of Polybutylene sebacate through M8 considering different surface area ($R^2 \geq 0.98$).

Among the most favorable models, M3 and M23 resulted to be inconsistent with the laboratory data of T4 ($R^2 = 94\%$) and T7 ($R^2 = 92\%$) treatments. On the other hand, other models exhibited identical capabilities. For example, the M1, M8, and M9 had almost equal capabilities due to having almost the same RMSE and R^2 values. Moreover, no significant differences were observed between M9 and M21 as far as statistical criteria were concerned. The M9 however was selected

as the best model for estimating the methane kinetics of all 9 treatments over time due to the simplicity of the model. The M9 model, which is appropriate for enzyme kinetics, possess fixed inflexion point with various curve shapes (Wang et al., 2011). This model exhibited a decrease in residuals as the incubation time progressed (Huhtanen et al., 2008). As a result of the considerable incubation time in the study, the fit performance of the M9 is deemed reliable. Huhtanen and colleagues (2008) reported that M9 series models had the highest gas yield. An overestimation of this parameter as well as underestimation of fractional rate was observed, though (Huhtanen et al., 2008). In another study that was performed recently, M21 had the best fit to data in the kinetic study of antibiotics inhibition in the AD of dairy manure (Andriamanohiarisoamanana et al., 2020).

There is an assumption that Gompertz models are capable to define the methane production rate as proportional to substrate level as well as microbial mass (Schofield et al., 1994). Thereby, M5, M12, and M14 models were mainly used to explain the methane production of different substrates. For example, in a study for describing the co-digestion kinetics of food waste with poultry manure, the modified Gompertz model presented better results than the Logistic model (Deepanraj et al., 2017). The use of the Gompertz model, especially for PHBV, has already been validated in such a way that it can predict methane production based on the surface area and PS (Ryan et al., 2017). Likewise, García-Depraect et al. (2022) reported 0.99 goodness of fit for PHB and PHBV.

However, current findings do not support previous researches in this area. The M5, M12, and M14 models were seldom practical to be a good indicator for the AD kinetics of starch-based bioplastic due to $PP \neq 0$. The important point was that these models only in ISR: 2 could predict the methane production rate with a negligible PP and an acceptable approximation ($p \leq 0.05$). Also, it should be noted that the lack of lag phase made their statistical results identical more or less. Therefore,

it is recommended that researchers be used M12 exclusively at the ISR: 2 due to the possibility of lag phase calculation.

Calculating the kinetic parameters is valuable for BMP tests, particularly biodegradation patterns (Ware & Power, 2017). Table 3 shows the values of M9 coefficients along with their standard deviation for each treatment. a , b and c represent cumulative methane production, time at $\frac{a}{2}$ respectively, and shape parameter. The foremost result from this table is that all the treatments were significant at the 1% significance level. According to this model, the highest amounts of methane were obtained for T3 and T6, which were about 15% and 8% more than their laboratory value, respectively. c could be helpful when dealing with substrates that accumulate intermediate fermenters like fatty acids (Ware & Power, 2017). In principle $c \leq 1$ implies that the fractional degradation rate decreases continuously while $c > 1$ indicates this rate increases first and later decreases during digestion (France et al., 2000). This is in line with the results provided in Table 3 and Figure 2(b). An explanation for this interpretation of c can be associated with the multiplied microbial population and colonization to create a 'biofilm' before the maximum degradation rate was reached (Groot et al., 1996). Also it could be attributed to the accessibility of the substrate, and completion of the rapidly degradable substrate as well (Huhtanen et al., 2008). It can be further derived from the table that with increasing ISR, the shape parameter decreased for all treatments except T3. On the other side with increasing PS at each level of the ISR, the value of b increased except for T8.

The cumulative diagram of each treatment along with the upper (UB) and lower (LB) boundaries is plotted in Figure 1. To predict this production process, laboratory data in triple replications (R1 to R3) were fitted to M9. This simple model provided a proper visual fit and was able to predict the methane production of all treatments with a suitable approximation ($R^2 > 0.97$). Nevertheless,

the visual fit for T1 still revealed an overestimation of methane production between the 8th and 10th day, indicating defective conversion of short chain fatty acids (Streitwieser & Cabezas, 2018) and consequently the inhibition of methanogens. Intense production between the first and fourth day supports this result. Rapid solubilization of starch could be a plausible reason that was also reported for thermoplastic starch: Polyvinyl alcohol blends (Russo et al., 2009). Fast hydrolysis and acidogenesis, and VFA accumulation in the last step of methanogenesis is also stated (Streitwieser & Cabezas, 2018). Degradation patterns for T4 and T7 were elongated S-shape, which can be attributed to the low bioavailability of the substrate and insufficient count of microorganisms for decomposing polymer, causing low degradation in the initial step. All other treatments had a reverse L-shape that accounts for the high daily production in the initial phase (Ware & Power, 2017).

The cumulative productions of treatments are shown in Figure 2 (a). As it can be observed, T3 and T6 produced the highest yield of methane. T6 produced less methane than T3 until the 9th day, following which, the yield produced gradually exceeded T3. It is apparent that a lag phase could be omitted for describing the kinetics of methane production for starch-based bioplastics. Lack of lag phase has a direct relationship with the nature of the substrate (hydrophilicity of starch polymer), the microbial species, and the amount of inoculum added (France et al., 2000). Generally, during the first step of biodegradation, discoloration happened and the polymer surface was broken with abiotic factors (heat and water) that facilitated the conversion of large molecules to smaller oligomer and monomers by enzymes and free radicals (primary degradation). After reduction of polymer molecular size, they passed the cell walls of microbes through specific membrane carriers or biotransformation reactions (mineralization). During this stage biogas is produced (Lucas et al., 2008; Muniyasamy et al., 2017). The first step could not be demonstrated

by the proposed model due to lack of lag phase, although mineralization has been shown thoroughly.

Figure 2 (b) also shows the methane production rate from the treatments over 26 days. Three phases can be distinguished in sigmoid gas production curves: 1) stage of slow or absent gas production (initial stage), 2) rapid gas production stage (exponential stage), and 3) stage during which the quantity of gas production is slowed down and at last reaches zero (asymptotic stage). Throughout the initial phase, water uptake, binding, and colonization of insoluble substrates by rumen microbes occur. Once the substrate is saturated with microbes or enzymes, the exponential gas production step is achieved. During this stage, the foremost simply degradable part of the insoluble substrate is first broken down and leaves a much less digestible substrate. Eventually, undegradable materials remain and the rate of gas production drops to zero (Beuvink & Kogut, 1993). In other words, the last two stages were corresponding to the attacking of microorganisms to amorphous and semicrystalline/crystalline zones of starch polymer, respectively (Li et al., 2007). Thus, a preliminary growth in the fractional rate reflects particle hydration, microorganism attachment, and increase in microbial population count which are attributed to a rise in substrate accessibility, while the decrease could be justified by the imposition of chemical and structural constraints (France et al., 2000). The methane production rate in most treatments, except PS: 7.87 mm, was close to the cellulose one until the third day. This result correlated favorably with Gómez & Michel Jr (2013) study during the first 7 days of Plastarch biodegradation (Gómez & Michel Jr, 2013). The maximum rates of biodegradation for trials were between 22 and 40 mL CH₄/g.VS.day. These values were much higher than Wang et al. (2018) study for Poly(3-hydroxybutyrate-co-3-hydroxyhexanoate), but they were lower for T5, T8 and T9 trials comparing to Ryan et al. (2017) research. Likewise, this parameter for T1, T2 and T3 was higher when it comes to large PS of

García-Depraect et al. (2022) study (0.5-1mm). T6 in comparison to T3 had lower access of microorganisms to the nutrients in bioplastics (starch) and a lower surface area of bioplastic particles as well. An upshot of this was that the production rate of T6 to the second day was lower than T3. In the initial stage of the process (after the second day) a sharp drop in production rate was observed for T1. Meanwhile, the percentage of methane in biogas decreased to 42% (see supplementary material). Gradually, however, it regained its methane production after the 8th day and took a steady trend. Easily degraded material, as well as insufficient ISR, incurred the connotation of this decreasing trend (Zhang et al., 2019). Though all the PSs had unique thicknesses, the specific surface area (SSA) differed widely. For instance, the SSA of PS:0.72 was 1.85 times higher than PS:4.3. This ratio was 1.1 for PS:4.3 by comparison of PS:7.87. It is worthy to mention that the calculation of SSA was based on the hypothesis that all of the surfaces were smooth squares without any roughness. In reality, bioplastic surfaces have porosity that the application of mechanical pretreatment intensifies. Thus higher specific surface area and the greater availability of these particles to microorganisms could be another reason that led to rapid hydrolysis of these fine particles and accumulation of fatty acids (Ryan et al., 2017). The final pH of T1 (6.6) was in favor of this founding. Weiwei and colleagues (2016) put forward similar results between the 3rd and 8th days on starch / PVA compounds with natural amylose (Weiwei et al., 2016). The researchers also reported that volatile fatty acid (VFA) production was high on days 1 to 4, although there was no inhibition (Guo et al., 2011). Thus, great care must be taken when dealing with bioplastics that are plausible for large amount production of VFAs as if these intermediate products had a determinant role in the validation of kinetic models for bioplastic AD (Ryan et al., 2017).

3.3. MLP neural network design

Although NLR could model changes in methane production over time with high accuracy and appropriate R^2 , it depended only on the time variable. Also, an NLR model was used for the treatments, even though different coefficients were obtained for each treatment. For these reasons, the MLP-ANN was used as another alternative to have a model that can estimate the kinetics of methane production in terms of PS and ISR changes over time. To design an MLP neural network, selecting the appropriate training algorithm is mandatory. The training algorithm finds the relationship between independent and dependent variables according to the training process through repetition. Figure 3 shows the predicted RMSE result of the methane production for train, test, and total steps using 12 common types of ANN training algorithms. The algorithms were sorted by the total RMSE value. The Levenberg-Marquardt training algorithm (trainlm) showed improved predictive performance than other algorithms. Of course, the Bayesian Regularization training algorithm (trainbr) had a slight discrepancy from the trainlm training algorithm however, the trainlm training algorithm was used to train MLP neural network. This algorithm was of Quasi-Newton class, which overcame the complexity of computing the Hessian matrix issue.

The performance result of using different datasets is detailed in Table 4. These datasets were randomly selected. This table showed a steady improvement in test accuracy as the training set is increased. Also small differences were observed for 80% and 60% of data. It means that with decreasing the dataset, there were no RMSE intense changes. Thus, the generalization of the model was verified. In the end, 80% of total data were used to learn the network and the remaining of it were enough for testing the model. In addition to the type of training algorithm, the number of neurons in the hidden layer is another important parameter in the design of the MLP neural network. The results of the RMSE prediction changes in two stages of the ANN according to the number of neurons has been demonstrated (see supplementary material). The network prediction

performance improved by increasing the number of neurons to 15 in the hidden layer for both training and testing. In other words, the RMSE value decreased from about 14 to approximately 3 and 1 for test and train steps respectively, but then no substantial change was observed. Fewer numbers of neurons were used to prevent the increase in computational volume and to have a simpler neural network. Therefore, 15 neurons in the hidden layer were used to design the MLP-ANN. Figure 4 shows the graph of laboratory data versus the predicted data by the model in two stages of training and testing. These data were slightly different from the $y = x$ line and there was an exceptional agreement between the model prediction and the experimental data. Consequently, the model was of good quality. The process of producing methane from starch-based bioplastics over time in each ISR is illustrated in Figure 5. MLP-ANN well predicted the PP parameter as well as cumulative methane production. It could also be inferred from the figure that methane production increased with increasing ISR, and particles between 1 and 5 mm had the highest methane production. Moreover, the gradient of the graph tended to be high in the early stage of degradation, as there was a considerable amount of gas production, which resulted in the lack of lag phase. Subsequently the diagram approached the upper asymptote with a constant increase as the substrate depleted. Thereby, all of the biological findings in NLR analysis could be described based on this figure.

3.4. Comparison of NLR with MLP-ANN

This section provides a comparison of the best NLR and MLP-ANN identified. Unlike the NLR model, a single model that included all the parameters of PS, ISR, and time was achieved using the MLP-ANN. In other words, one model replaced the previous nine models to define the kinetics of methane production. Following this advantage, statistical criteria have indicated that the MLP-ANN was a superior model to monitor biodegradation over time. Table 5 illustrates data regarding

statistical results for NLR and the best dataset of MLP-ANN. The most conspicuous observation to emerge from the data comparison was that both of them had a good agreement with the data. Though the R^2 results were relatively close for the two models, MLP-ANN had the edge on M9 concerning EF. Also, MLP-ANN displayed marginally lower RMSE and TSSE compare to M9.

3.5. Sensitivity analysis

Sensitivity analysis was used to investigate the impact of model input parameters on methane production. For this purpose, by deleting each of the model parameters and re-executing it, the effect of the deleted parameter on the accuracy of the model was evaluated. The sensitivity coefficient of the MLP model is shown in Figure 6. Evidently, time had the greatest effect on kinetics, which is evidenced by the fact that faster digestion rates corresponded to higher substrate consumption by microorganisms. This figure also confirms the authors' previous results on the impact of ISR being a more influential parameter on AD performance than PS reduction (Ebrahimzade et al., 2021).

4. Conclusion

In this study, 9 models that had good potential for investigating the kinetics of the AD of starch-based bioplastics were introduced. Among them, M9 had the best performance in estimating the methane production kinetics of each of the 9 treatments over time. On the other hand, the MLP-ANN was used as another alternative to cover the deficiencies of NLRs. This model had an agreement in enough depth ($R^2 = 0.99$, $PP = 0$) and was taken as the superior model. It could be suggested that future researches be focused on the validation of the proposed models using different bioplastic substrates.

E-supplementary data for this work can be found in e-version of this paper online.

Acknowledgments

This study was financially supported by Ferdowsi University of Mashhad (FUM), Iran (Grant No. 51329). The authors would also like to thank UNESCO for providing some of the instruments used in this study under the grant number No. 18-419 RG, which was funded by the World Academy of Sciences (twas).

References

1. Abunama, T., Othman, F., Ansari, M., El-Shafie, A. 2019. Leachate generation rate modeling using artificial intelligence algorithms aided by input optimization method for an MSW landfill. *Environmental Science and Pollution Research*, **26**(4), 3368-3381.
2. Andriamanohiarisoamanana, F.J., Ihara, I., Yoshida, G., Umetsu, K. 2020. Kinetic study of oxytetracycline and chlortetracycline inhibition in the anaerobic digestion of dairy manure. *Bioresource Technology*, **315**, 123810.
3. Archontoulis, S.V., Miguez, F.E. 2015. Nonlinear regression models and applications in agricultural research. *Agronomy Journal*, **107**(2), 786-798.
4. Bátori, V., Åkesson, D., Zamani, A., Taherzadeh, M.J., Horvath, I.S. 2018. Anaerobic degradation of bioplastics: A review. *Waste management*, **80**, 406-413.
5. Beuvink, J., Kogut, J. 1993. Modeling gas production kinetics of grass silages incubated with buffered ruminal fluid. *Journal of Animal Science*, **71**(4), 1041-1046.
6. Chinaglia, S., Tosin, M., Degli-Innocenti, F. 2018. Biodegradation rate of biodegradable plastics at molecular level. *Polymer Degradation and Stability*, **147**, 237-244.
7. Cho, H., Moon, H., Kim, M., Nam, K., Kim, J. 2011. Biodegradability and biodegradation rate of poly (caprolactone)-starch blend and poly (butylene succinate) biodegradable polymer under aerobic and anaerobic environment. *Waste management*, **31**(3), 475-480.

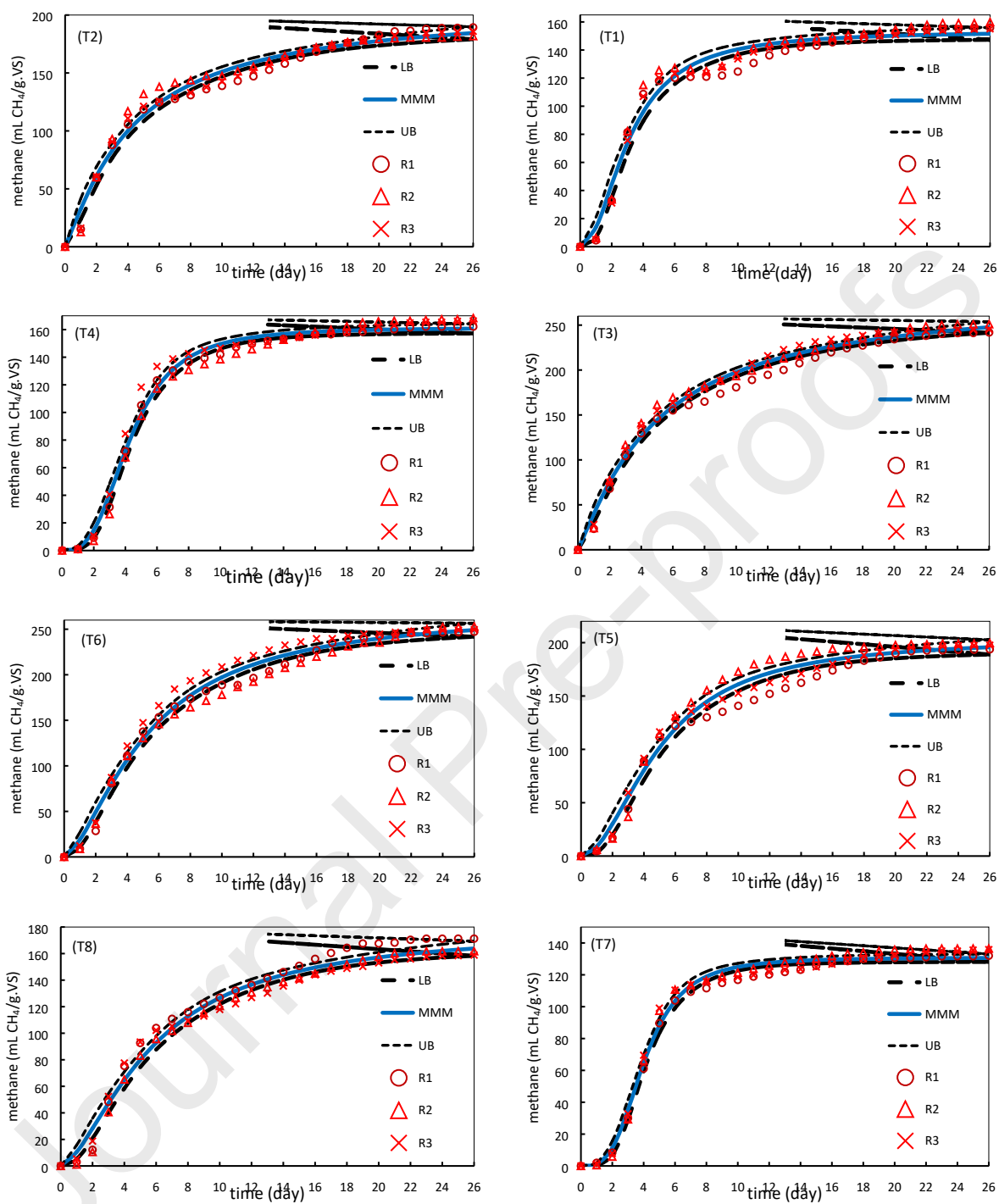
8. Davis, G., Song, J. 2006. Biodegradable packaging based on raw materials from crops and their impact on waste management. *Industrial crops and products*, **23**(2), 147-161.
9. Deepanraj, B., Sivasubramanian, V., Jayaraj, S. 2017. Effect of substrate pretreatment on biogas production through anaerobic digestion of food waste. *International Journal of Hydrogen Energy*, **42**(42), 26522-26528.
10. Ebrahimzade, I., Ebrahimi-Nik, M., Rohani, A., Tedesco, S. 2021. Higher energy conversion efficiency in anaerobic degradation of bioplastic by response surface methodology. *Journal of Cleaner Production*, **290**, 125840.
11. Europeanbioplastics. 2020. Bioplastics market data.
12. Europeanbioplastics. 2016. Fact Sheets - What are Bioplastics?, <https://www.european-bioplastics.org/bioplastics/>, [accessed 8 September 2019].
13. France, J., Dijkstra, J., Dhanoa, M., Lopez, S., Bannink, A. 2000. Estimating the extent of degradation of ruminant feeds from a description of their gas production profiles observed in vitro: derivation of models and other mathematical considerations. *British Journal of Nutrition*, **83**(2), 143-150.
14. García-Depraect, O., Lebrero, R., Rodriguez-Vega, S., Bordel, S., Santos-Beneit, F., Martínez-Mendoza, L.J., Börner, R.A., Börner, T., Muñoz, R. 2022. Biodegradation of bioplastics under aerobic and anaerobic aqueous conditions: Kinetics, carbon fate and particle size effect. *Bioresource Technology*, **344**, 126265.
15. Gómez, E.F., Michel Jr, F.C. 2013. Biodegradability of conventional and bio-based plastics and natural fiber composites during composting, anaerobic digestion and long-term soil incubation. *Polymer Degradation and Stability*, **98**(12), 2583-2591.
16. Groot, J.C., Cone, J.W., Williams, B.A., Debersaques, F.M., Lantinga, E.A. 1996. Multiphasic analysis of gas production kinetics for in vitro fermentation of ruminant feeds. *Animal Feed Science and Technology*, **64**(1), 77-89.

- 1 17. Guo, H.-n., Wu, S.-b., Tian, Y.-j., Zhang, J., Liu, H.-t. 2020. Application of machine learning
2 methods for the prediction of organic solid waste treatment and recycling processes: A review.
3 *Bioresource Technology*, 124114.
- 4 18. Guo, M., Trzcinski, A., Stuckey, D., Murphy, R. 2011. Anaerobic digestion of starch–polyvinyl
5 alcohol biopolymer packaging: Biodegradability and environmental impact assessment.
6 *Bioresource technology*, **102**(24), 11137-11146.
- 7 19. Holliger, C., Alves, M., Andrade, D., Angelidaki, I., Astals, S., Baier, U., Bougrier, C., Buffière,
8 P., Carballa, M., De Wilde, V. 2016. Towards a standardization of biomethane potential tests.
9 *Water Science and Technology*, **74**(11), 2515-2522.
- 10 20. Huhtanen, P., Seppala, A., Ahvenjarvi, S., Rinne, M. 2008. Prediction of in vivo neutral detergent
11 fiber digestibility and digestion rate of potentially digestible neutral detergent fiber: Comparison
12 of models. *Journal of animal science*, **86**(10), 2657-2669.
- 13 21. Khamis, A. 2005. Nonlinear growth models for modeling oil palm yield growth. *J. of mathematics*
14 *and statistics*, **1**(3), 225-233.
- 15 22. Li, W., Corke, H., Beta, T. 2007. Kinetics of hydrolysis and changes in amylose content during
16 preparation of microcrystalline starch from high-amylose maize starches. *Carbohydrate Polymers*,
17 **69**(2), 398-405.
- 18 23. Lucas, N., Benaïme, C., Belloy, C., Queneudec, M., Silvestre, F., Nava-Saucedo, J.-E. 2008.
19 Polymer biodegradation: Mechanisms and estimation techniques—A review. *Chemosphere*, **73**(4),
20 429-442.
- 21 24. Maleki, E., Bokhary, A., Liao, B. 2018. A review of anaerobic digestion bio-kinetics. *Reviews in*
22 *Environmental Science and Bio/Technology*, **17**(4), 691-705.
- 23 25. Massardier-Nageotte, V., Pestre, C., Cruard-Pradet, T., Bayard, R. 2006. Aerobic and anaerobic
24 biodegradability of polymer films and physico-chemical characterization. *Polymer Degradation*
25 *and Stability*, **91**(3), 620-627.

26. Mohee, R., Unmar, G., Mudhoo, A., Khadoo, P. 2008. Biodegradability of biodegradable/degradable plastic materials under aerobic and anaerobic conditions. *Waste Management*, **28**(9), 1624-1629.
27. Muniyasamy, S., Muniyasamy, S., John, M.J., John, M.J. 2017. Biodegradability of Biobased Polymeric Materials in Natural Environments. *Handbook of Composites from Renewable Materials*, 625-653.
28. Nair, N., Sekhar, V., Nampoothiri, K., Pandey, A. 2017. Biodegradation of biopolymers. in: *Current Developments in Biotechnology and Bioengineering*, Elsevier, pp. 739-755.
29. Nielfa, A., Cano, R., Fdz-Polanco, M. 2015. Theoretical methane production generated by the co-digestion of organic fraction municipal solid waste and biological sludge. *Biotechnology Reports*, **5**, 14-21.
30. Piemonte, V. 2011. Bioplastic wastes: the best final disposition for energy saving. *Journal of Polymers and the Environment*, **19**(4), 988-994.
31. Quecholac-Piña, X., Hernández-Berriel, M.d.C., Mañón-Salas, M.d.C., Espinosa-Valdemar, R.M., Vázquez-Morillas, A. 2020. Degradation of Plastics under Anaerobic Conditions: A Short Review. *Polymers*, **12**(1), 109.
32. Rafiq, M., Bugmann, G., Easterbrook, D. 2001. Neural network design for engineering applications. *Computers & Structures*, **79**(17), 1541-1552.
33. Rohani, A., Abbaspour-Fard, M.H., Abdolahpour, S. 2011. Prediction of tractor repair and maintenance costs using Artificial Neural Network. *Expert Systems with Applications*, **38**(7), 8999-9007.
34. Russo, M.A., O'Sullivan, C., Rounsefell, B., Halley, P.J., Truss, R., Clarke, W.P. 2009. The anaerobic degradability of thermoplastic starch: Polyvinyl alcohol blends: Potential biodegradable food packaging materials. *Bioresource Technology*, **100**(5), 1705-1710.

35. Ryan, C.A., Billington, S.L., Criddle, C.S. 2017. Assessment of models for anaerobic biodegradation of a model bioplastic: Poly (hydroxybutyrate-co-hydroxyvalerate). *Bioresource technology*, **227**, 205-213.
36. Saghour, M., Abdi, R., Ebrahimi-Nik, M., Rohani, A., Maysami, M. 2020. Modeling and optimization of biomethane production from solid-state anaerobic co-digestion of organic fraction municipal solid waste and other co-substrates. *Energy Sources, Part A: Recovery, Utilization, and Environmental Effects*, 1-17.
37. Schofield, P., Pitt, R., Pell, A. 1994. Kinetics of fiber digestion from in vitro gas production. *Journal of animal science*, **72**(11), 2980-2991.
38. Shah, A.A., Hasan, F., Hameed, A., Ahmed, S. 2008. Biological degradation of plastics: a comprehensive review. *Biotechnology advances*, **26**(3), 246-265.
39. Shojaeimehr, T., Rahimpour, F., Khadivi, M.A., Sadeghi, M. 2014. A modeling study by response surface methodology (RSM) and artificial neural network (ANN) on Cu²⁺ adsorption optimization using light expended clay aggregate (LECA). *Journal of Industrial and Engineering Chemistry*, **20**(3), 870-880.
40. Shrestha, A., van-Eerten Jansen, M.C., Acharya, B. 2020. Biodegradation of bioplastic using anaerobic digestion at retention time as per industrial biogas plant and international norms. *Sustainability*, **12**(10), 4231.
41. Stoddard, I. 2010. Communal Polyethylene Biogas Systems: Experiences from on-farm research in rural West Java, Vol. Doctoral dissertation, Uppsala University.
42. Streitwieser, D.A., Cabezas, I.C. 2018. Preliminary study of biomethane production of organic waste based on their content of sugar, starch, lipid, protein and fibre. *Chemical Engineering Transactions*, **65**, 661-666.
43. Wang, M., Tang, S., Tan, Z. 2011. Modeling in vitro gas production kinetics: derivation of logistic–exponential (LE) equations and comparison of models. *Animal Feed Science and Technology*, **165**(3-4), 137-150.

- 1 44. Wang, S., Lydon, K.A., White, E.M., Grubbs III, J.B., Lipp, E.K., Locklin, J., Jambeck, J.R. 2018.
2 Biodegradation of poly (3-hydroxybutyrate-co-3-hydroxyhexanoate) plastic under anaerobic
3 sludge and aerobic seawater conditions: gas evolution and microbial diversity. *Environmental*
4 *science & technology*, **52**(10), 5700-5709.
- 5 45. Ware, A., Power, N. 2017. Modelling methane production kinetics of complex poultry
6 slaughterhouse wastes using sigmoidal growth functions. *Renewable Energy*, **104**, 50-59.
- 7 46. Weiwei, L., Juan, X., Beijiu, C., Suwen, Z., Qing, M., Huan, M. 2016. Anaerobic biodegradation,
8 physical and structural properties of normal and high-amylose maize starch films. *International*
9 *Journal of Agricultural and Biological Engineering*, **9**(5), 184-193.
- 10 47. Yagi, H., Ninomiya, F., Funabashi, M., Kunioka, M. 2012. Anaerobic biodegradation of poly (lactic
11 acid) film in anaerobic sludge. *Journal of Polymers and the Environment*, **20**(3), 673-680.
- 12 48. Yagi, H., Ninomiya, F., Funabashi, M., Kunioka, M. 2009. Anaerobic biodegradation tests of poly
13 (lactic acid) and polycaprolactone using new evaluation system for methane fermentation in
14 anaerobic sludge. *Polymer Degradation and Stability*, **94**(9), 1397-1404.
- 15 49. Zhang, W., Heaven, S., Banks, C.J. 2018. Degradation of some EN13432 compliant plastics in
16 simulated mesophilic anaerobic digestion of food waste. *Polymer Degradation and Stability*, **147**,
17 76-88.
- 18 50. Zhang, W., Torrella, F., Banks, C.J., Heaven, S. 2019. Data related to anaerobic digestion of
19 bioplastics: Images and properties of digested bioplastics and digestate, synthetic food waste recipe
20 and packaging information. *Data in brief*, **25**, 103990.



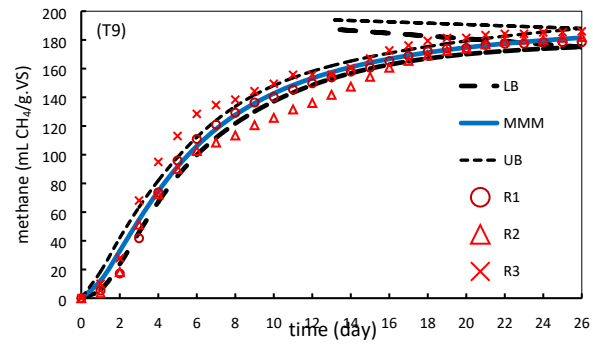


Figure 1: The diagrams of cumulative methane production of treatments using Modified MM (M9)

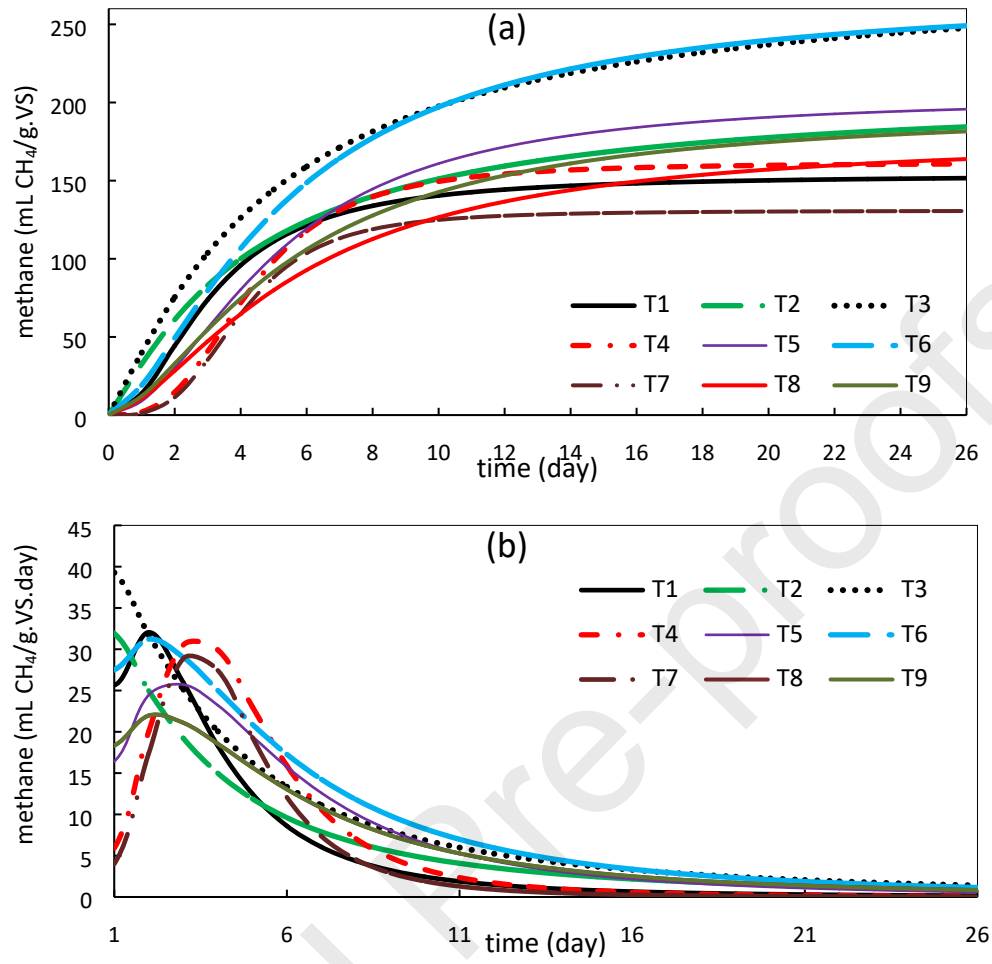


Figure 2: Cumulative (a) and rate (b) of methane production of samples mentioned in Table 1

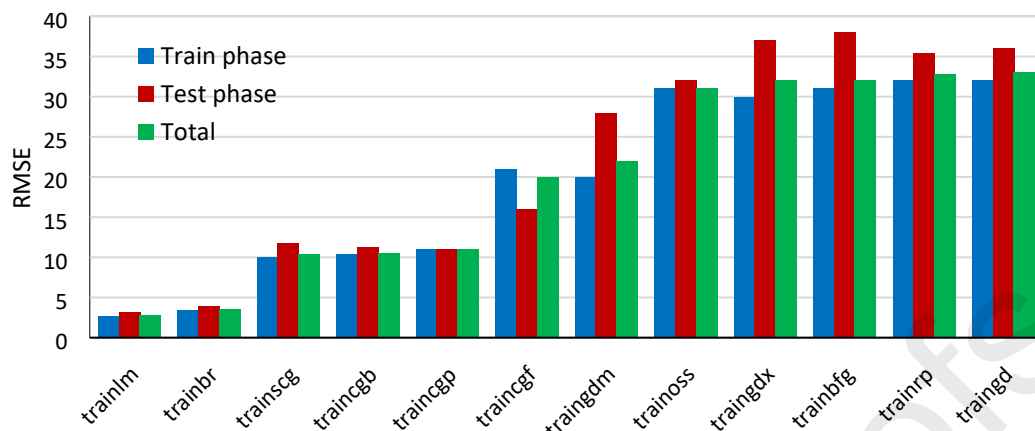


Figure 3: Performance of MLP-ANN training algorithms in predicting kinetics of methane production

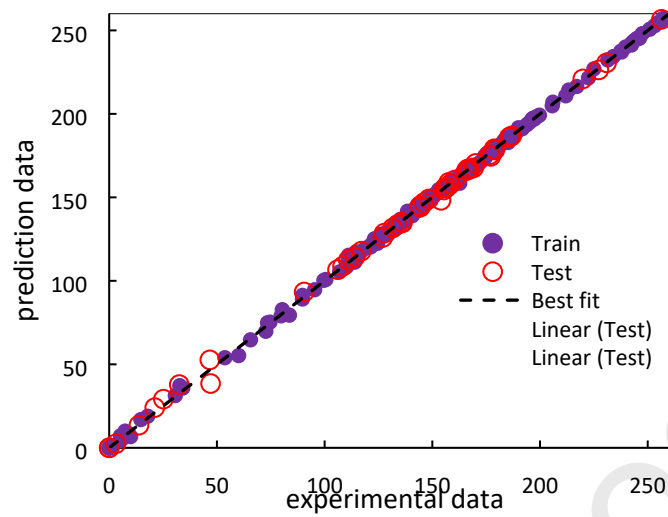


Figure 4: The result of evaluating the agreements between experimental methane production and their predicted values by the MLP-ANN

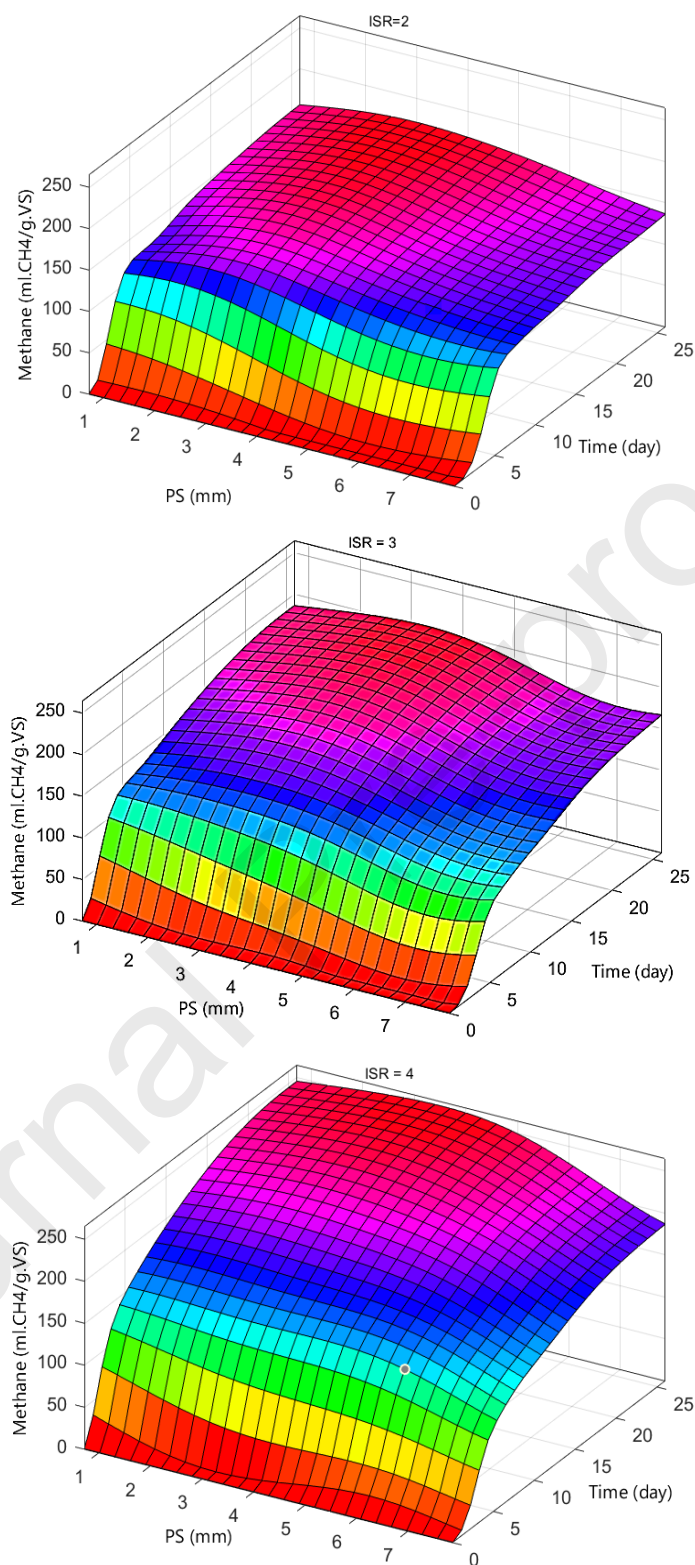


Figure 5: The kinetics of cumulative methane production over time in ISRs 2 (a), 3 (b), and 4 (c)

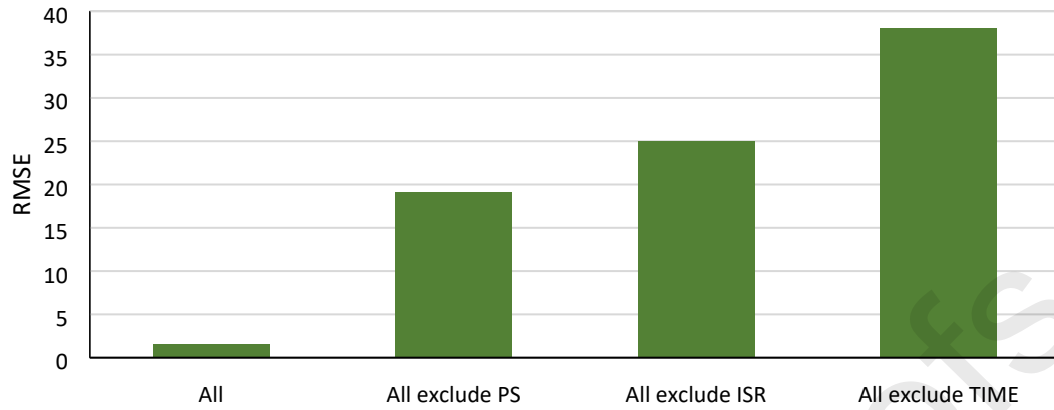


Figure 6: Sensitivity coefficient of independent parameters of MLP model in anaerobic digestion kinetics of starch-based bioplastics

1

Table 1. experimental treatments and their relevant symbols

PS (mm)	ISR	Treatment
0.72	2	T1
0.72	3	T2
0.72	4	T3
4.30	2	T4
4.30	3	T5
4.30	4	T6
7.87	2	T7
7.87	3	T8
7.87	4	T9

Table 2. NLRs for kinetic study

Name	Form	Model
Logistic-Exponential without LAG	$f(t) = a \frac{1 - \exp(-bt)}{1 + \exp(\ln\left(\frac{1}{d}\right) - bt)}$	M1
Logistic-Exponential with LAG	$f(t) = a \frac{1 - \exp(-b(t-c))}{1 + \exp(\ln\left(\frac{1}{d}\right) - b(t-c))}$	M2
Exponential without LAG	$f(t) = a(1 - \exp(-bt))$	M3
Exponential with LAG	$f(t) = a(1 - \exp(-b(t-c)))$	M4
Gompertz	$f(t) = a \exp(-\exp(1 - b(t-c)))$	M5
Logistic	$f(t) = a \frac{1}{1 + \exp(2 + b(c-t))}$	M6
Generalization of the Mitscherlich	$f(t) = a(1 - \exp(-b(t-c) - d(\sqrt{t} - \sqrt{c})))$	M7
Michaelis-Menten (MM)	$f(t) = a \frac{t^c}{t^c + b^c}$	M8
Modified MM	$f(t) = a \frac{t^c}{t^c + b}$	M9
Two-pool exponential	$f(t) = \sum_{i=1}^2 a_i(1 - \exp(-b_i(t-c)))$	M10
Two-pool logistic	$f(t) = \sum_{i=1}^2 a_i \frac{1}{(1 + \exp(2 - 4b_i(t-c)))}$	M11
Modified Gompertz	$f(t) = a \exp(-\exp(2.71 \frac{b}{a}(c-t) + 1))$	M12
Logistic	$f(t) = a \frac{1}{1 + b \exp(-ct)}$	M13
Gompertz	$f(t) = a \exp(-b \exp(-ct))$	M14
Richard	$f(t) = a \frac{1}{(1 + b \times \exp(-ct))^{1/d}}$	M15
Double-Sigmoid	$f(t) = a \frac{1}{1 + \exp(-(b + ct + dt^2 + et^3))}$	M16
Monomolecular- logistic	$f(t) = a(1 - \exp(-bt)) + \frac{c}{1 + \exp(-d(t-e))}$	M17
Chapman-Richard	$f(t) = a(1 - b \times \exp(-ct))^{(\frac{1}{1-d})}$	M18
Exponential-linear	$f(t) = \frac{a}{b} \times \ln(1 + \exp(b(t-ct)))$	M19
LinBiExp	$f(t) = a \times \ln(\exp(\frac{b(t-c)}{d})) + \exp(\frac{e(t-f)}{g}) + f$	M20
Cone	$f(t) = a(\frac{1}{1 + (bt)^{-c}})$	M21
Contois	$f(t) = a(1 - \frac{b}{ct + b - 1})$	M22
Fitzhugh	$f(t) = a(1 - \exp(-bt)^c)$	M23
France	$f(t) = \frac{a(1 - \exp^{-bt})}{(1 + c \exp^{-bt})}$	M24

Monod without LAG	$f(t) = a \frac{bt}{bt + 1}$	M25
Monod with LAG	$f(t) = a \frac{b(t - c)}{b(t - c) + 1}$	M26

1

Table 3: The values of Modified MM (M9) parameters for each treatment

coefficient	T1	T2	T3	T4	T5	T6	T7	T8	T9
<i>a</i>	154 ±	207 ±	284 ±	161 ±	204 ±	270 ±	131 ±	179 ±	196 ±
	1.65**	5.46**	6.98**	1.11**	6.63**	5.46**	0.75**	4.17**	4.61**
<i>b</i>	2.03 ±	1.16 ±	1.15 ±	3 ±	1.91 ±	1.55 ±	3.36 ±	1.59	1.61 ±
	0.12**	0.07**	0.06**	0.14**	0.12**	0.08**	0.15**	0.09**	0.1**
<i>c</i>	10.1 ±	5.34 ±	6.11 ±	79.9 ±	21.6 ±	13.1 ±	108 ±	15.9 ±	15.1 ±
	1.55**	0.4**	0.37**	16.5**	21.6**	1.49**	23.3**	2.11**	2.14**

1

Table 4: RMSE results of using different datasets in ANN steps

Dataset (percentage of total data)	Train	Test	Total
80%	1.22	2.49	1.55
60%	1.37	2.81	2.08
40%	3.06	5.26	4.51
20%	3.87	9.39	8.57

Table 5: statistical results of NLR and MLP-ANN

Criteria	NLR (M9)									MLP-ANN		
	T1	T2	T3	T4	T5	T6	T7	T8	T9	train	test	total
R ²	0.97	0.98	0.99	0.99	0.98	0.98	0.99	0.98	0.98	0.99	0.99	0.99
RMSE	10.44	8.29	7.73	6.06	9.37	9.54	4.44	6.99	8.53	1.22	2.49	1.55
TSSE	8825	5565	4835	2969	7106	7369	1599	3953	5895	289	296	586
EF	0.94	0.97	0.99	0.99	0.98	0.98	0.99	0.98	0.98	0.99	0.99	0.99
PP	0	0	0	0	0	0	0	0	0	0	0	0

CRediT author statement

Manuscript title: *Towards monitoring biodegradation of starch-based bioplastic in anaerobic condition: finding a supreme kinetic model*

All persons who meet authorship criteria are listed as authors, and all authors certify that they have participated sufficiently in the work to take public responsibility for the content, including participation in the concept, design, analysis, writing, or revision of the manuscript. Furthermore, each author certifies that this material or similar material has not been and will not be submitted to or published in any other publication before its appearance in the *Journal of Bioresource Technology*.

Yours faithfully,

Mohammadali Ebrahimi-Nik, PhD

Corresponding author, on behalf of all authors

Declaration of interests

☒ The authors declare that they have no known competing financial interests or personal relationships that could have appeared to influence the work reported in this paper.

☐ The authors declare the following financial interests/personal relationships which may be considered as potential competing interests:

1



2

3

4

5

6

7

Highlights:

8

- The kinetics of bioplastics biodegradation have not been dealt with in depth.

9

- 9 out of 26 analyzed NLRs, were proper for monitoring the AD of bioplastics.

10

- M9 selected as the best NLR owing to the simplicity and good statistical criteria.

11

- MLP-ANN had an agreement in enough depth to data and picked as the superior model.

12